Structural properties of strained epitaxial La 1+δ CrO 3 thin films

Dong Han, Mohamed Bouras, Claude Botella, Aziz Benamrouche, Bruno Canut, Geneviève Grenet, Guillaume Saint-Girons, Romain Bachelet

Structural properties of strained epitaxial $La_{1+\delta}CrO_3$ thin films

Dong Han[1], Mohamed Bouras[1], Claude Botella[1], Aziz Benamrouche[1], Bruno Canut[2], Geneviève Grenet[1], Guillaume Saint-Girons[1], Romain Bachelet[1,a)]

[1]Institut des Nanotechnologies de Lyon – INL CNRS UMR 5270, Université de Lyon, Ecole Centrale de Lyon, 36 avenue Guy de Collongue, 69134 Ecully, France

[2]Institut des Nanotechnologies de Lyon – INL CNRS UMR 5270, Université de Lyon, INSA de Lyon, 7 avenue Jean Capelle, 69621 Villeurbanne, France

[a)] Electronic mail: romain.bachelet@ec-lyon.fr

Epitaxially strained $La_{1+\delta}CrO_3$ (LCO) thin films, with δ ranging between −0.25 (Cr-rich) and 0.25 (La-rich), were grown on $SrTiO_3$(001) substrates by solid-source molecular beam epitaxy (MBE). The effect of the cationic-stoichiometry deviation (δ) on the structural properties (surface structure, morphology, terminations and unit-cell parameters) is reported. Whereas deviation from stoichiometry does not significantly affect the structural quality (all films keep a perovskite structure, are epitaxial, atomically flat, fully strained, and present mosaicity below 0.1°), increasing $|\delta|$ leads to an increase of the out-of-plane lattice parameter and of the unit-cell volume. These results are of importance for further studies on structure-properties relationships in the view to build enhanced LCO-based devices.

I. INTRODUCTION

Perovskite oxides with general formula ABO_3 (A being an alkaline metal, alkaline earth metal, or lanthanide, and B being a 3*d* transition metal) have attracted much attention in the past several decades due to their remarkable physical and chemical properties such as ferroelectricity, ferromagnetism, thermoelectricity, in addition to chemical stability and flexibility, as well as physical tunability and couplings, that make them very appealing for diverse applications[1,2]. The lanthanum chromite, $LaCrO_3$ (LCO), is an antiferromagnetic insulator (T_N ~ 290 K) with a charge transfer gap of 3.3 eV[3,4]. LCO exhibits an orthorhombic bulk structure (space group *Pbnm*) with lattice parameters a = 5.513 Å, b = 5.473 Å and c = 7.759 Å at room temperature and ambient pressure[5]. However, it can be viewed as a pseudocubic lattice cell with a_{pc} = 3.885 Å[6,7], structurally compatible with other functional perovskite oxides. The properties of LCO that can be tuned by forming solid solutions, enable its use in many different key applications and devices (*e.g.* solid-oxide fuel cells[8], memories[9,10], catalysis[11], as well as water splitting[12] and *p*-type transparent conductivity and thermoelectricity[13]). Previous studies have shown the impact of pressure, strain, chemical composition, couplings and atomically-defined interfaces on the physical properties (magnetic, electronic, optical, phononic, etc.) of LCO-based materials[14,15,16,17,18,19,20,21,22,23,24]. LCO has been mainly studied theoretically[17,18,20] or experimentally in the form of bulk powders or polycrystalline films[8,9,11,14,15,24]. However, highly demanding applications, as well as refined property tuning based on advanced control of the structural properties require state-of-the-art growth of epitaxial LCO films, as introduced by Ueda *et al*. with ferromagnetic epitaxial [$LaFeO_3$/$LaCrO_3$] superlattices grown by pulsed laser deposition (PLD)[19]. Qiao *et al*.[7] have introduced a successful epitaxial growth of stoichiometric $LaCrO_3$ by molecular beam epitaxy (MBE), allowing studies of interface physics for instance[16,21,22]. However, the effect of the cationic-stoichiometry deviation (δ) in $La_{1+\delta}CrO_3$ on structural properties has

been studied only within a restricted range close to the stoichiometry ($-0.15 < \delta < 0.1$, or also noted $0.85 < x = 1+\delta = La/Cr < 1.1$ for La_xCrO_3)[25], whereas it can be of critical importance for properties and applications. They have mainly focused on the formation of point defects, surface segregation and cationic intermixing at the interface with $SrTiO_3$(001) substrate. A clear structural trend with a wider stoichiometry deviation is lacking. It is well known that stoichiometry deviation tends to enlarge the unit-cell volume through the formation of charged ionic vacancies in the lattice, and thus enlarge the out-of-plane lattice parameter (and consequent tetragonality) in strained epitaxial ABO_3 films, like in the reference $SrTiO_3$ (STO)[26,27,28]. For instance, the deviation of the cationic stoichiometry in STO epitaxial films can be large while maintaining a perovskite structure and can greatly impact their physical properties such as the electronic and phononic transport[29,30,31]. Similarly, Kan *et al.*[32] have shown that the structural and ferroelectric properties depend on the cationic stoichiometry in $BaTiO_3$ epitaxial thin films. Likewise, Qiao *et al.*[33] focused on the effects of stoichiometry deviation on the structural properties and intermixing at the $LaAlO_3$/STO(001) interface, and Warusawithana *et al.*[34] have shown that off-stoichiometry (Al-rich $LaAlO_3$ films) is required to obtain the two-dimensional electron gas at this interface.

In this study, epitaxially-strained $La_{1+\delta}CrO_3$ thin films were grown with high quality on STO(001) substrates by MBE with δ widely varying in the ±0.25 range. The impact of large cationic-stoichiometry deviation (δ) on LCO structural properties has been investigated. Particularly, the surface structure, morphology, terminations, lattice cell parameters and crystalline quality of the LCO thin films are shown and discussed.

II. EXPERIMENTAL

About 15 nm thick epitaxial $La_{1+\delta}CrO_3$ (LCO) thin films were grown on single-crystalline STO(001) substrates (MaTecK GmbH) by solid-source MBE in a UHV chamber with a base pressure $\leq 1\times10^{-9}$ Torr. La and Cr were evaporated from effusion cells in codeposition, with a growth rate of ~0.1 nm/min. The fluxes were measured before the growth using a Bayard-Alpert (BA) gauge (after subtraction of the background pressure), and checked using a quartz crystal microbalance (QCM) (Fig. SI 1). The molecular oxygen partial pressure $P(O_2)$ was kept constant at 1×10^{-7} Torr during the growth, and the growth temperature was set to 700°C. The STO substrates were annealed for 15 minutes before starting the growth. Reflection high-energy electron diffraction (RHEED) was used to *in-situ* monitor the LCO growth and the surface quality. The LCO epitaxial films were grown by layer-by-layer mode (Fig. SI 2). All the films were grown on as-received STO(001) substrates, except for one additional stoichiometric LCO film (δ = 0) grown on a TiO_2-terminated STO(001) substrate. The standard preparation for TiO_2-terminated STO(001) substrates consists in *i*) 10 min of ultrasonic immersion in deionized water (to enhance the subsequent acid etching), *ii*) 20s etching in buffered HF solution (to have only remaining TiO_2 termination), *iii*) rinsing abundantly in deionized water (to avoid residual etchant yielding etching pits) and drying with nitrogen, and *iv*) annealing in air at 1000°C for 1 hour (to flatten the TiO_2-terminated terraces)[35,36].

Atomic force microscopy (AFM) working in tapping mode was used to measure the surface morphology, mean roughness, as well as chemical contrast by phase-shift imaging[37,38,39,40] (Fig. 2 and Fig. SI 3). Film structure was investigated by X-ray diffraction (XRD) using a Rigaku Smartlab diffractometer equipped with a high-brilliance rotating anode, and a double-crystal Ge(220) monochromator. The crystalline orientation, out-of-plane cell parameters and relative crystalline quality were examined through 2θ-ω scans and ω-scans (Fig. 3 and Fig. SI 7). In-plane lattice parameters were obtained from reciprocal space

maps (RSM) around the asymmetric (103) reflection (Fig. 4). X-ray reflectivity (XRR) was also used to measure the thickness of the films (Fig. SI 6). Rutherford backscattering spectrometry (RBS), using a 2 MeV He^+ beam incident at 6° with a 172° scattering angle, was used to check the cationic stoichiometry of the films, which was in perfect agreement with the XRD results within the instrumental uncertainties (Fig. SI 4). X-ray photoelectron spectroscopy (XPS) spectra were acquired using monochromatic Al Kα radiation ($h\nu$ = 1486.6 eV) at normal emission to check the near-surface region of the films (Fig. SI 5).

III. RESULTS AND DISCUSSION

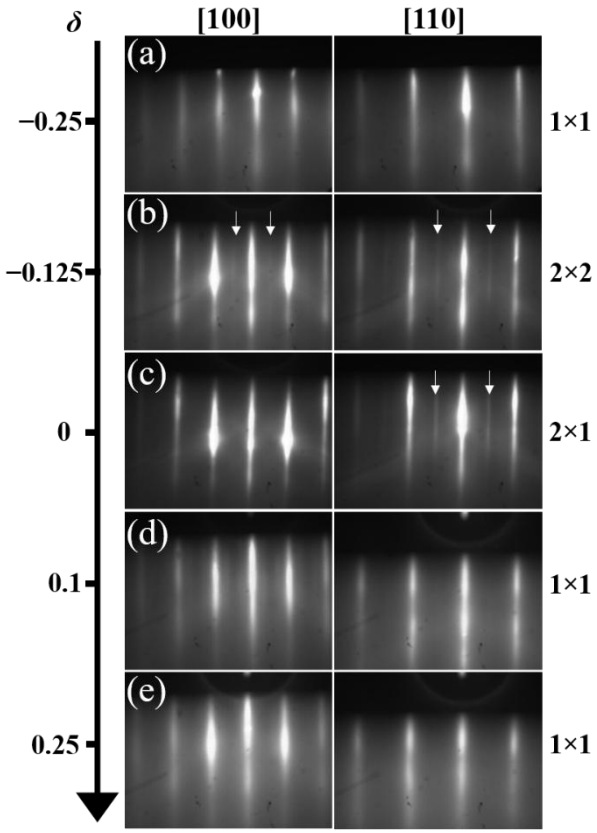

FIG. 1 (single column). RHEED patterns recorded along the <100> and <110> azimuths (around 200°C, $P(O_2) = 1\times10^{-9}$ Torr) after growth of the $La_{1+\delta}CrO_3$ films, (a) $\delta = -0.25$; (b) $\delta = -0.125$; (c) $\delta = 0$; (d) $\delta = 0.1$ and (e) $\delta = 0.25$. The vertical white arrows indicate 2nd order reflections demonstrating

surface reconstruction in the considered azimuth. Corresponding surface reconstruction is indicated on the right of the RHEED patterns for each composition.

RHEED patterns along both high-symmetry <100> and <110> in-plane crystallographic directions are shown after the growth of LCO thin films (Fig. 1). All the RHEED patterns present well contrasted streak lines meaning that all the films are epitaxial with flat surface. However, for $|\delta| = 0.25$ (Fig. 1a and 1e), the streaks are slightly blurred and the background is brighter than that observed for samples with lower $|\delta|$, revealing larger crystalline disorder. For $\delta = -0.125$ (slightly Cr-rich LCO film, Fig. 1b) and $\delta = 0$ (stoichiometric LCO film, Fig. 1c), the streaks are sharp along both azimuths, indicating that the surface is well ordered. Additionally, for both these samples, a 2^{nd} order streaky reflection along the <110> direction (indicated by arrows in Fig. 1) is observed. A weak 2^{nd} order streaky reflection also appears along the <100> azimuth for $\delta = -0.125$ whereas only 1^{st} order reflection is observed along this azimuth at $\delta = 0$, which indicates a 2×2 and a 2×1 surface reconstruction for the slightly Cr-rich LCO film ($\delta = -0.125$, Fig. 1b) and the stoichiometric film ($\delta = 0$, Fig. 1c), respectively. In contrast, when $\delta = 0.1$ (slightly La-rich LCO film, Fig. 1d) only 1^{st} order streaks are visible indicating the absence of surface reconstruction.

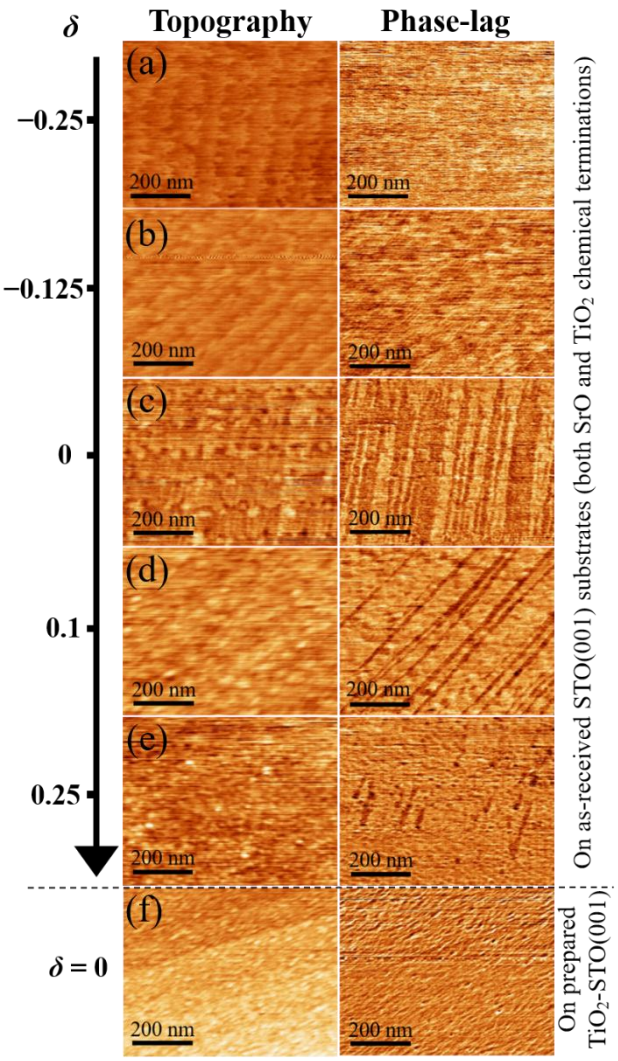

FIG. 2 (single column). 1x1 μm^2 AFM topographic (left panel) and phase-lag (right panel) images of the LCO thin films grown on as-received STO(001) substrate with (a) $\delta = -0.25$, (b) $\delta = -0.125$, (c) $\delta = 0$, (d) $\delta = 0.1$ and (e) $\delta = 0.25$. (f) LCO thin film grown on prepared TiO_2-terminated STO(001) substrate with $\delta = 0$.

AFM images of the film surface are shown in Fig. 2. The left panel and the right panel present the topographic images and the phase-lag images, respectively. In agreement with RHEED patterns (Fig. 1) and XRR analysis (Fig. SI 6), all the topographic images reveal smooth surfaces with root-mean-square (rms) roughness less than 0.3 nm. Atomic steps and terraces can be clearly observed for the Cr-rich LCO films ($\delta < 0$, Fig. 2a and 2b), and are still distinguishable for the stoichiometric film ($\delta = 0$, Fig. 2c). For the La-rich LCO films ($\delta > 0$,

Fig. 2d and 2e), the "steps and terraces" morphology becomes unclear, and completely disappears at δ = 0.25 (Fig. 2e), even if the surfaces remain globally flat (rms roughness is about 0.25 nm at δ = 0.25). The La-rich surface could present 2D-islands of La_2O_3 randomly distributed on the surface, even if the XPS spectra does not show any evidence of secondary phase in the near surface region (Fig. SI 5)[25].

The phase-lag images reveal chemical contrasts on flat surfaces, although phase-lag contrast may also appear at step edges due to sharp height differences[37,38,39,40] In Fig. 2, strong persistent phase-lag contrast appears at the surface of the stoichiometric film (δ = 0) in which the contrast is roughly half-tone (Fig. 2c). This contrast indicates a double termination (CrO_2 and LaO) at the surface of the stoichiometric film, due to the replication during stoichiometric 2D-growth of the double termination initially present at the surface of unprepared STO substrate[40]. The half unit-cell steps measured on topographic image at the phase-lag contrast location is consistent with this interpretation (Fig. SI 3). This chemical contrast at the film surface decreases and disappears when $|\delta|$ increases, confirming the dominance of one cation at the surface of non-stoichiometric films. The AFM analysis carried out on the film grown on a prepared TiO_2-terminated STO(001) substrate further confirms this assumption. In that case, step heights of unit-cell height are measured (Fig. SI 3) and no contrast is observed in the phase-lag image (Fig. 2f), indicating a single chemical termination, most probably the CrO_2-termination if no switching of chemical termination occurs during growth, which seems to be the case since no delay is observed in the RHEED intensity oscillations at the first stage of layer-by-layer growth (Fig. SI 2).

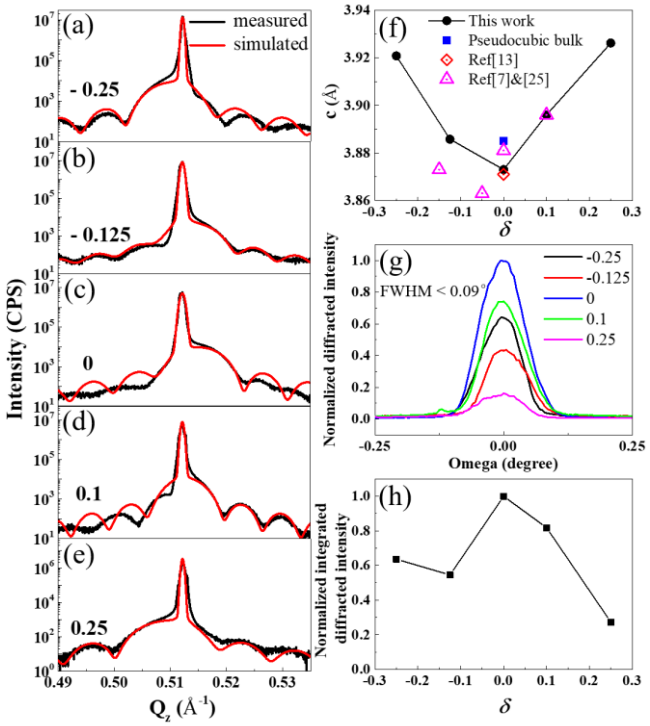

FIG. 3 (single column). XRD characterizations. (a-e) 2θ-ω scans near the (002) Bragg reflections of LCO thin films and STO substrates for (a) $\delta = -0.25$; (b) $\delta = -0.125$; (c) $\delta = 0$; (d) $\delta = 0.1$ and (e) $\delta = 0.25$. (f) Out-of-plane lattice cell parameter as a function of the cationic-stoichiometry deviation δ. (g) ω-scans around the LCO (002) reflection for all the films, normalized to the stoichiometric film ($\delta = 0$). (h) Normalized integrated diffracted intensity of the ω-scans shown in (g) as a function of δ.

The structural properties of all LCO films have been investigated by XRD. Wide 2θ-ω scans (10-80°) reveal only diffraction peaks corresponding to the {00l} reflections of the LCO films and STO(001) substrates (Fig. SI 7), showing that no other orientation or phase than LCO (00l) are present in the epitaxial films. Cationic intermixing at the interface with STO and secondary phase formation, which are dependent on the growth conditions and STO substrate quality, are not observed here by XRD (and XPS) although a few La-rich precipitates could be present at the nanometer scale close to the interface[25]. The presence of Pendellosung fringes around the diffraction peaks of the films attest their high crystalline quality. Fig. 3a-e show the XRD 2θ-ω scans around the (002) reflections of the LCO films

and STO substrates plotted in reciprocal space units. The LCO (002) reflection is very close to that of STO substrate and appears as a shoulder of the substrate peak (Fig. 3 and Fig. SI 5). Qualitatively, the position of the film reflection decreases in Q_z while deviating from the stoichiometry, which means that the out-of-plane cell parameter of the LCO film (c_{LCO}) increases with cationic-stoichiometry deviation. Both Cr-rich and La-rich films exhibit larger c_{LCO} than that of the stoichiometric LCO film, in agreement with other perovskite oxide films such as $SrTiO_3$[26,27,28]. This standard trend is also observed by Qiao *et al.*, but with a c_{LCO} minimum (less than 3.87 Å) shifted at slightly Cr-rich films ($\delta = -0.05$) and not at the stoichiometry ($\delta = 0$)[25]. This small composition shift (5%) with our results could be due to *i*) the uncertainty in the determination of composition and film lattice parameter, and *ii*) to the ratio and distribution of point cationic defects (vacancy, anti-site) in the films.

Quantitatively, c_{LCO} has been extracted here from fits of the XRD spectra (Fig. 3a-e), and is shown as a function of δ in Fig. 3f, together with the results of the Chambers' group on fully-strained epitaxial LCO films for comparison[7,13,25]. Our values range from 3.873 Å to 3.926 Å. Our minimal value, recorded for the stoichiometric film, is c_{LCO} = 3.873 Å which is in good agreement with the most recent results of the Chambers' group[13], although different values (from 3.871 to 3.881 Å) are reported in different articles from this group on fully-strained stoichiometric LCO epitaxial film on STO(001) substrate[7,13,25]. Around the stoichiometry, lattice parameters are lower than the LCO pseudocubic bulk value (3.885 Å, blue dotted line), indicating reduced c_{LCO} (−0.3%) owing to the in-plane tensile stress exerted by STO(001) substrate (relative in-plane tensile strain $\mathcal{E} = 0.51\%$)[41]. The out-of-plane lattice cell parameter increases up to almost 3.93 Å for clearly non-stoichiometric films: 3.92 Å for $\delta = -0.25$ and 3.926 Å for $\delta = 0.25$. In such cases, these high c_{LCO} values, superior to the substrate lattice parameter, are partly due to in-plane compressive strain of the epitaxial films, in addition to the effect of cationic-stoichiometry deviation it-self. For $\delta = 0.1$ (slightly La-

rich film), c_{LCO} = 3.896 Å, in very good agreement with Qiao's results[25]. For δ = −0.125 (slightly Cr-rich), c_{LCO} = 3.886 Å, which is slightly larger than the Qiao's reported value (~3.873 Å for δ = −0.15)[25].

The ω-scans measured for all the films around the LCO (002) reflection are shown in Fig. 3g. The mosaicity of the films (full width at half maximum, FWHM, of these curves) is below 0.09°, comparable to that of the single-crystalline STO substrates, confirming the high-quality of the films with a low level of defects. However, Figure 3h shows that the diffracted intensity progressively decreases with δ, most probably due to the introduction of cationic vacancies in the lattice (modifying the structural factor) which must permit to keep high-quality perovskite structure in all cases even with such large (25%) cationic variations.

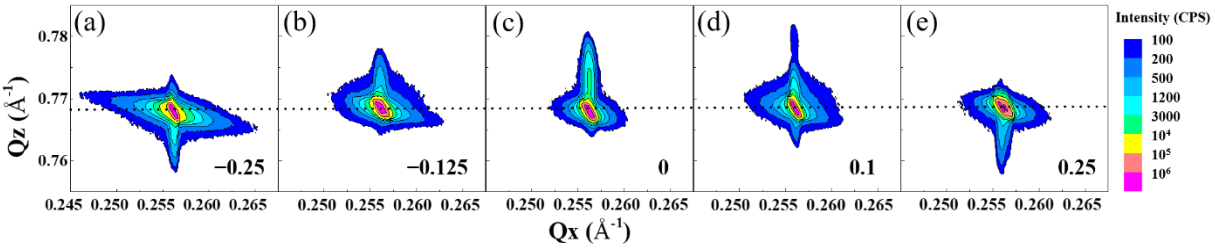

FIG. 4 (double column if possible). Reciprocal space maps around the asymmetric (103) reflection of the LCO thin films and STO substrate, for (a) δ = −0.25, (b) δ = −0.125, (c) δ = 0, (d) δ = 0.1 and (e) δ = 0.25. The dotted line indicates the Q_z position of the STO substrate related to its out-of-plane lattice parameter (c_{STO}).

The in-plane lattice parameters of the LCO films and the associated anisotropic strain have been measured by XRD reciprocal space mapping around asymmetrical reflection. Fig. 4 shows the reciprocal space maps (RSMs) acquired around the asymmetric (103) reflection of LCO films and STO substrate. The shoulder of the nodes corresponding to the LCO thin films is shifted along Q_z depending on chemical composition consistently with the 2θ-ω scans,

confirming the variation of c_{LCO} shown in Fig. 3. By contrast, the LCO (103) node are aligned vertically with the substrate node, indicating that the in-plane lattice parameters of the LCO thin films (a_{LCO}) are equal to the STO(001) lattice cell parameter (3.905 Å). All LCO films are fully coherently strained to the substrates, confirming that the critical thickness (t_c) from which an epitaxial strain relaxation occurs is well above the thickness of our thin films. This is consistent both with the low lattice mismatch of LCO/STO(001) heteroepitaxy (0.51%)[41] and with previous experimental results (t_c > 50 nm)[7].

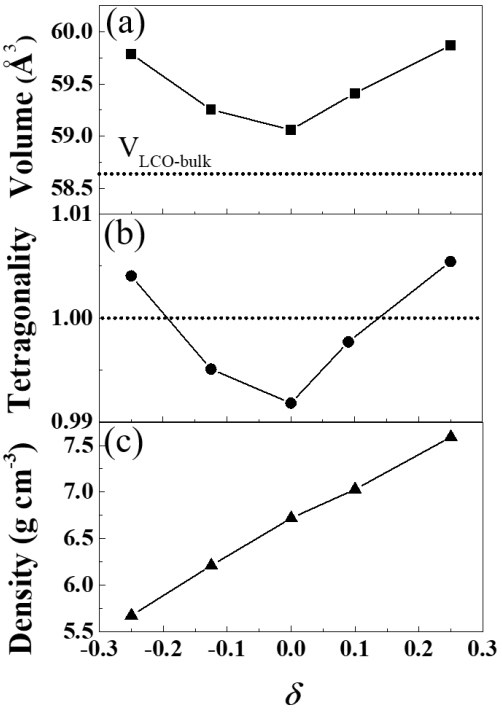

FIG. 5 (single column). Dependence on δ of (a) the lattice unit-cell volume, (b) the tetragonality c/a, and (c) the density of LCO thin films.

From the measured out-of-plane and in-plane lattice cell parameters (c and a), the unit-cell volume can be extracted and plotted as a function of cationic-stoichiometry deviation (Fig. 5a). The unit-cell volume is found to be in-between 59 and 60 Å^3 within the composition range. A trend similar to the evolution of c with δ is observed since a remains constant with a

minimum at stoichiometry. Cationic-stoichiometry deviation might generate point defects such as cationic vacancies that induce expansion of the unit-cell volume from electrostatic repulsions near these charged ionic defects. Around the stoichiometry, for $\delta = -0.125$, 0 and 0.1, the LCO films exhibit values of *a* that exceed *c*, induced by the heteroepitaxial in-plane tensile stress. However, for larger stoichiometric deviation, when $\delta = \pm 0.25$, it turns to in-plane compressive stress since *c* is larger than *a*, which means that the corresponding bulk pseudocubic lattice parameter in such cases is larger than that of the STO substrate (> 3.905 Å). The tetragonality (*c*/*a*) is found to vary between 0.99 and 1.01 and is plotted as a function of δ in Fig. 5b. The density of all LCO films were extracted from unit-cell volume and chemical composition, and is plotted as a function of δ in Fig. 5c. Film density has an approximate linear increasing trend with δ due to the progressive introduction of La with larger atomic mass in the crystal lattice.

Regarding the literature on the impact of pressure, strain, chemical composition, couplings and atomically-defined interfaces on the physical properties of LCO-based materials (magnetic, electronic, optical, phononic, etc.)[14,15,16,17,18,19,20,21,23,24], the progressive change of chemical composition, lattice parameters and epitaxial strain observed in this study may change the physical properties of the LCO films and could be further exploited to build enhanced or novel LCO-based devices.

IV. CONCLUSIONS

In summary, high-quality ~15 nm thick (00*l*)-oriented $La_{1+\delta}CrO_3$ epitaxial thin films with $-0.25 \leq \delta \leq 0.25$ were grown on STO(001) substrates by MBE. Despite such large composition range, all films conserve the perovskite structure, are atomically flat, epitaxial and fully strained, with mosaicity below 0.1°. Any secondary phase has been observed with

the different structural characterization techniques used here (RHEED, XRD, XPS, AFM). The out-of-plane lattice parameter and unit-cell volume reach a minimum at the cationic stoichiometry (3.873 Å and 59.06 $Å^3$, respectively) and increase when deviating from it. The diffracted intensity slightly decreases with δ, most probably due to the introduction of cationic vacancies in the lattice, which must permit to keep high-quality perovskite structure in all cases even with such large (25%) cationic variations. These results are of high interest for further understanding the interplay between the structural and physico-chemical properties in order to build enhanced or novel LCO-based devices.

ACKNOWLEDGMENTS

Financial support from the European Commission through the project TIPS (grant reference H2020-ICT-02-2014-1-644453) and the French research national agency (ANR) through the project MITO (grant reference ANR-17-CE05-0018) is acknowledged. The China Scholarship Council (CSC) is acknowledged for the grant of D. Han. The authors are also grateful to the joint laboratory RIBER-INL and P. Regreny and J. B. Goure for the MBE technical support.

REFERENCES

[1] *Thin films and heterostructures for oxide electronics*, edited by S. B. Ogale (Springer, New York, 2005).

[2] *Functional oxides*, edited by D. W. Bruce, D. O'Hare, and R. I. Walton (John Wiley & Sons, Padstow, 2010).

[3] I. Weinberg, and P. Larssen, Nature **192**, 445 (1961).

[4] T. Arima, Y. Tokura, and J. B. Torrance, Phys. Rev. B **48**, 17006 (1993).

[5] J. Yang, Acta Crystallogr. Sect. B **64**, 281 (2008).

[6]T. Hashimoto, K. Takagi, K. Tsuda, M. Tanaka, K. Yoshida, H. Tagawa, and M. Dokiya, J. Electrochem. Soc. **147**, 4408 (2000).

[7]L. Qiao, T. C. Droubay, M. E. Bowden, V. Shutthanandan, T. C. Kaspar, and S. A. Chambers, Appl. Phys. Lett. **99**, 061904 (2011).

[8]P. Duran, J. Tartaj, F. Capel, and C. Moure, J. Eur. Ceram. Soc. **24**, 2619 (2004).

[9]W. J. Hu, L. Hu, R. H. Wei, X. W. Tang, W. H. Song, J. M. Dai, X. B. Zhu, and Y. P. Sun, Chinese Phys. Lett. **35**, 047301 (2018).

[10]X. Marti, I. Fina, C. Frontera, J. Liu, P. Wadley, Q. He, R. J. Paull, J. D. Clarkson, J. Kudrnovský, I. Turek, J. Kuneš, D. Yi, J. H. Chu, C. T. Nelson, L. You, E. Arenholz, S. Salahuddin, J. Fontcuberta, T. Jungwirth, and R. Ramesh, Nat. Mater. **13**, 367 (2014).

[11]K. Rida, A. Benabbas, F. Bouremmad, M. A. Peña, E. Sastre, and A. Martínez-Arias, Appl. Catal. B-Environ. **84**, 457 (2008).

[12]K. A. Stoerzinger, Y. Du, K. Ihm, K. H. L. Zhang, J. Cai, J. T. Diulus, R. T. Frederick, G. S. Herman, E. J. Crumlin, and S. A. Chambers, Adv. Mater. Interfaces **5**, 1701363 (2018).

[13]K. H. L. Zhang, Y. Du, A. Papadogianni, O. Bierwagen, S. Sallis, L. F. J. Piper, M. E. Bowden, V. Shutthanandan, P. V. Sushko, and S. A. Chambers, Adv. Mater. **27**, 5191 (2015).

[14]J. S. Zhou, J. A. Alonso, A. Muonz, M. T. Fernández-Díaz, and J. B. Goodenough, Phys. Rev. Lett. **106**, 057201 (2011).

[15]L. Qiao, H. Y. Xiao, S. M. Heald, M. E. Bowden, T. Varga, G. J. Exarhos, M. D. Biegalski, I. N. Ivanov, W. J. Weber, T. C. Droubay, and S. A. Chambers, J. Mater. Chem. C **1**, 4527 (2013).

[16]R. Colby, L. Qiao, K. H. L. Zhang, V. Shutthanandan, J. Ciston, B. Kabius, and S. A. Chambers, Phys. Rev. B **88**, 155325 (2013).

[17]B. Kim, P. Liu, J. M. Tomczak, and C. Franchini, Phys. Rev. B **98**, 075130 (2018).

[18]T. Mayeshiba, and D. Morgan, Phys. Chem. Chem. Phys. **17**, 2715 (2014).

[19]K. Ueda, H. Tabata, and T. Kawai, Science **280**, 1064 (1998).

[20]J. Hong, A. Stroppa, J. Íniguez, S. Picozzi, and D. Vanderbilt, Phys. Rev. B **85**, 054417 (2012).

[21]R. B. Comes, S. R. Spurgeon, S. M. Heald, D. M. Kepaptsoglou, L. Jones, P. V. Ong, M. E. Bowden, Q. M. Ramasse, P. V. Sushko, and S. A. Chambers, Adv. Mater. Interfaces **3**, 1500779 (2016).

[22]R. B. Comes, S. R. Spurgeon, D. M. Kepaptsoglou, M. H. Engelhard, D. E. Perea, T. C. Kaspar, Q. M. Ramasse, P. V. Sushko, and S. A. Chambers, Chem. Mater. **29**, 1147 (2017).

[23]P. V. Sushko, L. Qiao, M. Bowden, T. Varga, G. J. Exarhos, F. K. Urban III, D. Barton, and S. A. Chambers, Phys. Rev. Lett. **110**, 077401 (2013).

[24]B. Tiwari, A. Dixit, R. Naik, G. Lawes, and M. S. Ramachandra Rao, Appl. Phys. Lett. **103**, 152906 (2013).

[25]L. Qiao, K. H. L. Zhang, M. E. Bowden, T. Varga, V. Shutthanandan, R. Colby, Y. Du, B. Kabius, P. V. Sushko, M. D. Biegalski, and S. A. Chambers, Adv. Funct. Mater. **23**, 2953 (2013).

[26]C. M. Brooks, L. F. Kourkoutis, T. Heeg, J. Schubert, D. A. Muller, and D. G. Schlom, Appl. Phys. Lett. **94**, 162905 (2009).

[27]B. Jalan, R. Engel-Herbert, N. J. Wright, and S. Stemmer, J. Vac. Sci. Technol. A **27**, 461 (2009).

[28]B. Jalan, P. Moetakef, and S. Stemmer, Appl. Phys. Lett. **95**, 032906 (2009).

[29]T. Ohnishi, K. Shibuya, T. Yamamoto, and M. Lippmaa, J. Appl. Phys. **103**, 103703 (2008).

[30]E. Breckenfeld, R. Wilson, J. Karthik, A. R. Damodaran, D. G. Cahill, L. W. Martin, Chem. Mater. **24**, 331 (2012).

[31]C. M. Brooks, R. B. Wilson, A. Schäfer, J. A. Mundy, M. E. Holtz, D. A. Muller, J. Schubert, D. G. Cahill, and D. G. Schlom, Appl. Phys. Lett. **107**, 051902 (2015).

[32]D. S. Kan, and Y. Shimakawa, Appl. Phys. Lett. **99**, 081907 (2011).

[33]L. Qiao, T. C. Droubay, T. Varga, M. E. Bowden, V. Shutthanandan, Z. Zhu, T. C. Kaspar, and S. A. Chambers, Phys. Rev. B **83**, 085408 (2011).

[34] M. P. Warusawithana, C. Richter, J. A. Mundy, P. Roy, J. Ludwig, S. Paetel, T. Heeg, A. A. Pawlicki, L. F. Kourkoutis, M. Zheng, M. Lee, B. Mulcahy, W. Zander, Y. Zhu, J. Schubert, J. N. Eckstein, D. A. Muller, C. Stephen Hellberg, J. Mannhart, and D. G. Schlom, Nat. Commun. **4**, 2351 (2013).

[35]M. Kawasaki, K. Takahashi, T. Maeda, R. Tsuchiya, M. Shinohara, O. Ishiyama, T. Yonezawa, M. Yoshimoto, and H. Koinuma, Science **266**, 1540 (1994).

[36]G. Koster, B. L. Kropman, G. J. H. M. Rijnders, D. H. A. Blank, and H. Rogalla, Appl. Phys. Lett. **73**, 2920 (1998).

[37]R. García, R. Magerle, and R. Perez, Nat. Mater. **6**, 405 (2007).

[38]R. Bachelet, F. Sánchez, J. Santiso, C. Munuera, C. Ocal, and J. Fontcuberta, Chem. Mater. **21**, 2494 (2009).

[39]R. Bachelet, C. Ocal, L. Garzón, J. Fontcuberta, and F. Sánchez, Appl. Phys. Lett. **99**, 051914 (2011).

[40]C. Ocal, R. Bachelet, L. Garzón, M. Stengel, F. Sánchez, and J. Fontcuberta, Chem. Mater. **24**, 4177 (2012).

[41]The relative in-plane epitaxial strain ($\mathcal{E}$) due to the lattice mismatch (f) are defined here as: $\mathcal{E} = (a_{film} - a_{bulk}) / a_{bulk}$, and $f = (a_{sub} - a_{bulk}) / a_{bulk}$, where a_{film} is the measured in-plane lattice parameter of the LCO film, a_{bulk} the bulk lattice parameter of pseudo-cubic

LCO, and a_{sub} the lattice parameter of the substrate. Please note that $\mathcal{E} = f$ for fully strained epitaxial films ($a_{film} = a_{sub}$).